The synergistic effects of the constant region and variable heavy chain families of multimeric immunoglobulin M on its interaction with Fc-mu receptor and antigen

Wei-Li Ling[1], Samuel Ken-En Gan[1,2,3,4]*

[1]Antibody & Product Development Lab, Wenzhou-Kean University, Wenzhou 325000, Zhejiang Province, China
[2]Zhejiang Bioinformatics International Science and Technology Cooperation Center, Wenzhou-Kean University, Wenzhou 325000, Zhejiang Province, China
[3]Wenzhou Municipal Key Lab of Applied Biomedical and Biopharmaceutical Informatics, Wenzhou-Kean University, Wenzhou 325000, Zhejiang Province, China
[4]James Cook University, Singapore 387380, Singapore

*__Correspondence:__ Samuel Ken-En Gan, Zhejiang Bioinformatics International Science and Technology Cooperation Center, Wenzhou-Kean University, 88 Daxue Road, Ouhai District, Wenzhou 325000, Zhejiang Province, China. samgan@apdskeg.com
__Academic Editor:__ Buyong Ma, Shanghai Jiaotong University, China

Abstract

__Aim:__ As the primary response antibody with increasing use as a therapeutic immunoglobulin (Ig) format, IgM is also the largest antibody structure among the five major human isotypes. Spontaneously formed pentamers and hexamers of IgM have avidity effects that could compensate for weaker interactions in monomeric Igs. However, this advantage is counterbalanced by potential steric clashes when binding to multiple large antigens. Recent findings have challenged the expected canonical independence of Fc receptor (FcR) binding at the heavy chain constant (C)-region where the heavy chain C-region isotypes affected antigen binding at the variable (V)-regions, and the variable heavy (VH) families of the V-region affected FcR engagement at the antibody C-regions. With such effects found on other Ig isotypes, IgM candidates need to be investigated with regards to such effects, especially when considering its natural oligomerisation at the C-region that can amplify or modulate such allosteric effects.

__Methods:__ Through a panel of 14 recombinant complementarity determining regions (CDRs)-grafted trastuzumab and pertuzumab VH1-7 IgMs subjected to bio-layer interferometry measurements, the interactions with the antigen human epidermal growth factor receptor 2 (Her2), Fc-mu receptor (FcμR), and superantigen Protein L (PpL) were investigated.

__Results:__ Significant effects from the V-regions to mitigate FcμR binding and the IgM C-region bidirectional effect modulating Her2 antigen engagements at the V-regions were found. Additional modulatory effects from superantigen PpL binding on the V-region of the kappa chain (Vκ) mitigating antigen binding were also found, revealing possible novel mechanisms of antibody superantigens that can be moderated by the antibody VH frameworks.

Conclusions: These findings show that the oligomerisation of IgMs plays a significant role in FcμR, antigen, and superantigen binding that made IgM distinct from the other antibody isotypes and how these features should be considered during further development and protein engineering of IgM therapeutics.

Keywords

Introduction

Immunoglobulin M (IgM) is the primary response antibody isotype produced in the adaptive immune response [1] and is structurally the largest multimeric antibody among the five major human isotypes (IgM, IgA, IgD, IgG, and IgE). IgM oligomerises at its constant mu (Cμ) 4 domain of the heavy chain constant (C)-region tailpiece to form pentamers in the presence of joining (J)-chains and hexamers in the absence of J-chains [2, 3]. Through oligomerisation, IgM has avidity effects that can compensate for weaker antigen binding in monomeric antibody isotypes. In a study comparing pertuzumab and trastuzumab IgG1 and IgM binding to human epidermal growth factor receptor 2 (Her2) antigen, trastuzumab IgG1 showed stronger interactions with Her2 antigen than pertuzumab IgG1 [4, 5], but pertuzumab IgM showed stronger interaction with the Her2 antigen than trastuzumab IgM [6] due to the absence of significant steric clashes with binding multiple Her2 antigens [7]. Such effects may therefore limit the total occupancy of many multimeric IgM.

Apart from antigen binding, IgM further activates the downstream immune responses via cell surface receptors. There are a few receptors with an affinity for IgM. Two receptors, polymeric Ig receptor (pIgR) and receptor for IgA or IgM Fc-alpha/μ receptor (Fcα/μR), have multiple affinities for other antibody isotypes, while only one receptor, Fc-mu receptor (FcμR), has a sole affinity for IgM. FcμR [also known as TOSO or Fas apoptotic inhibitory molecule 3 (FAIM3)] is expressed on lymphoid cells such as B cells, T cells, and natural killer (NK) cells [8–10], and binds to the constant heavy (CH) 4 domain of IgM [11] to activate the immune effect via its Ig tail tyrosine (ITT) phosphorylation motif [12]. Recent studies showed that FcμR regulates cell survival when cross-linked by the IgM-antigen complex with other B-cell receptors [13].

With recent evidence demonstrating that antibody regions can exert allosteric effects on a distal region, where the variable (V)-regions, particularly the framework regions (FWRs) can mitigate the Fc receptor (FcR) binding sites (and thus FcR binding) at the heavy chain C-regions (CH) for IgA [14, 15], IgE [16], and IgG1 [17], a holistic [18] investigation for multimeric IgMs is timely. Considering the effects of non-antigen interacting regions such as the signal peptide [19] and variable heavy (VH)-variable light (VL) pairing [20], playing a role in antibody production and how the different regions, such as within the V- and C-regions, can come together to form amino acid stretches and pockets that can bind non-conventional antigens [21, 22], such interactions may underlie the mechanism of bacterial superantigen function on antibodies. Since microbial antibody superantigens bind to antibody regions [23, 24] to modulate antigen and receptor engagement [24], where Protein L (PpL) binds the variable region of the kappa (Vκ) light chain to elicit eventual immune escape, an in-depth investigation of such distal effects would also allow for future interventions to microbial superantigens permit immune escape.

Most current antibody therapeutics are IgGs, but the interest in the other isotype formats, such as IgM, has steadily increased in recent years. The contributory role of IgM in viral immunity was highlighted in the current severe acute respiratory syndrome coronavirus 2 (SARS-CoV-2) pandemic [25–28], and the promise of IgM as a therapeutic antibody was shown through the listed company IGM Biosciences currently with therapeutic IgM candidates undergoing phases 1 and 2 clinical trials (ClinicalTrials.gov Identifier: NCT04553692 and CT04082936) among others.

Given the promise of IgM antibodies and how such distal effects can eventually influence the development of IgM-based therapeutics, there is a need for whole antibody-level investigations. Thus, to investigate these effects, a panel of 14 recombinant VH family variants of trastuzumab and pertuzumab IgMs [where the

complementarity determining regions (CDRs) of the two clinical antibodies were grafted onto the VH1-7 family FWRs] [17, 19] were expressed, with their interactions to Her2 antigen and FcμR with PpL binding measured using bio-layer interferometry (BLI) for a systematic analysis of the V-region effects.

Materials and methods

The synthesis of the recombinant IgM VH1-7 variants

The recombinant IgM variants with trastuzumab [Protein Data Bank (PDB) 1N8Z] and pertuzumab (PDB 1S78) sequences were generated by subcloning the V-regions from the respective IgG1 VH1-7 variants from previous work [17, 19] to the IgM CH [5] and signal peptides [19, 29, 30]. The light chains were created by grafting the respective pertuzumab and trastuzumab Vκ1 sequence with the constant kappa (Cκ). Briefly, the plasmids (one for the heavy chain and one for the light chain) were transformed into DH5-alpha (DH5α) competent *Escherichia coli* [31] separately for plasmid production and purified using the column-based plasmid extraction [32].

The heavy and light chain plasmids (without J-chain) were then co-transfected into HEK293 cells using Polyethylenimine (PEI) MAX® [Catalogue (Cat): 24765-1, PolyScience]. The supernatant was harvested 14 days post-transfection and purified using the AKTA equipped with a PpL affinity column (Cat: 17547815, Cytiva) as previously optimised [20, 33]. The purified recombinant IgMs were then subjected to HiLoad Superdex 200 pg preparative size exclusion chromatography (SEC) columns (Cat: 28989335, Cytiva) to collect the predominate hexamer fractions as previously described [5], where only the multimeric fraction was collected for analysis.

BLI measurements

Equilibrium dissociation constant (KD) measurements of Fc-tagged human FcμR to recombinant pertuzumab and trastuzumab IgM variants were performed using the Octet Red96® system. Fc-tagged FcμR was immobilised on anti-human IgG Fc (AHC; Cat: 18-5060, Sartorius) biosensors with a 1.0 nM loading threshold setting. The loaded biosensors were then subjected to five concentrations (12.5, 25, 50, 100, and 200 nM) of multimeric IgM. For background noise subtraction, measurements were also performed without multimeric IgMs.

KD measurements of recombinant pertuzumab and trastuzumab IgM variants to Her2 antigen were performed using the Octet Red96® system using two capture methods. Recombinant pertuzumab and trastuzumab IgM variants were immobilised on PpL (Cat: 18-5085, Sartorius) biosensors with a 1.0 nM loading threshold setting. Similarly, recombinant pertuzumab and trastuzumab IgM variants were immobilised on streptavidin (SA; Cat: 18-5085, Sartorius) biosensors offline loaded with anti-IgM conjugate (Cat: 7102892500, Thermofisher Scientific) with 0.5 nM loading threshold setting (the lowest acceptable threshold due to the large size of the molecules and its cost). The loaded biosensors were then subjected to five concentrations (12.5, 25, 50, 100, and 200 nM) of Her2 antigen. For background noise subtraction, measurements were also performed without Her2.

The program and steps used were described as follows. The Octet Acquisition version 10.0 program was used to set the following steps for KD measurements: pre-conditioning [0.2 mol/L glycine, pH 1.52 and 10 × kinetic buffer (KB; Cat: 18-1105, Sartorius), 30 s]; initial baseline (10 × KB, 60 s); loading (ligands with specific threshold); baseline (10 × KB, 120 s); association (analyte, 300 s); dissociation (10 × KB, 600 s); regeneration (0.2 mol/L glycine, pH 1.52 and 10 × KB, 30 s). The KD values were calculated and populated based on the association rate constant (k_a) and dissociation rate constant (k_d) values using the data analysis v10.0 program using the 1:1 fitting model as was performed in all our previous work on the other isotypes, including that of IgM [5]. KD, k_a, k_d, and R^2 analysis were populated by the program. All measurements were performed in triplicates [4, 5, 14–17, 19, 21, 22, 24].

Results

BLI measurements of FcµR to pertuzumab and trastuzumab IgM variants

To measure the distal allosteric effects of the VH FWRs family to the FcµR binding site of IgM CH, seven VH family variants of both trastuzumab and pertuzumab were recombinantly stitched to the IgM C-region (Figure S1). Given that no J-chain was co-expressed, hexamers were expected to be the predominant oligomers, and this was also supported by the relatively single monomeric peak from the SEC (Figures S2 and S3) and electron microscopy (EM) data (Figure S4).

All the pertuzumab VH1-7 variants (Figure 1) bound to FcµR except for Pertuzumab (P) VH2, which had a very poor response R^2 value of 0.216. For the responsive PVH IgMs, the KD ranged from 29.73 nM to 267.6 nM, with the strongest binder as PVH1, followed by PVH7, 4, 3, 6, and PVH5 as the weakest binder.
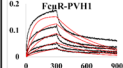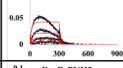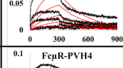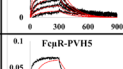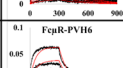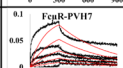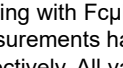
Construct	KD (nM)	k_a (1/Ms) 10^4	k_d (1/s) 10^{-4}	R^2	
PVH1	29.73 ± 0.47	12.96 ± 0.17	32.16 ± 0.25	0.892	FcµR-PVH1
PVH2	PR	PR	PR	0.216	FcµR-PVH2
PVH3	135.09 ± 6.31	5.35 ± 0.15	50.23 ± 0.66	0.822	FcµR-PVH3
PVH4	76.38 ± 2.20	12.31 ± 0.28	102.62 ± 1.56	0.889	FcµR-PVH4
PVH5	267.6 ± 20.55	6.58 ± 0.24	123.41 ± 2.39	0.833	FcµR-PVH5
PVH6	165.93 ± 6.19	16.98 ± 0.41	133.23 ± 1.82	0.910	FcµR-PVH6
PVH7	47.35 ± 1.29	5.55 ± 0.10	21.62 ± 0.25	0.837	FcµR-PVH7

Figure 1. BLI measurement of pertuzumab IgM variants (PVH1-7) interacting with FcµR bound to AHC biosensor. KD, k_a, k_d, R^2, and fitting curves are shown. PR indicates poor responses where the measurements have a poor R^2 value are shown in red. The x-axis and y-axis of the graph represent time (s) and response (nM), respectively. All values are rounded off to 2 decimal places. Triplicate experiments were performed, and standard errors were reported. PR: poor responses

The trend for trastuzumab HVH1-7 variants (Figure 2) was different from the pertuzumab variants despite having very minor differences of only a few amino acids at the CDRs. For example, Trastuzumab HVH1 IgM did not bind to FcµR, having a poor response R^2 value of 0.585. The rest of the HVH IgM KDs ranged from 23.29 nM to 210.47 nM (relatively similar to the PVH IgMs). The best to the weakest binder for the HVHs were in the order of HVH7, 3, 5, 6, 4, and 2.
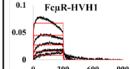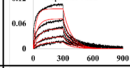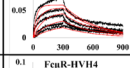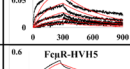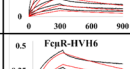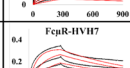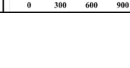
Construct	KD (nM)	k_a (1/Ms) 10^4	k_d (1/s) 10^{-4}	R^2	
HVH1	PR	PR	PR	0.585	FcµR-HVH1
HVH2	210.47 ± 9.16	6.09 ± 0.16	107.00 ± 1.37	0.905	FcµR-HVH2
HVH3	33.53 ± 0.63	9.58 ± 0.13	26.05 ± 0.23	0.877	FcµR-HVH3
HVH4	66.91 ± 1.44	3.13 ± 0.06	20.71 ± 0.20	0.904	FcµR-HVH4
HVH5	48.8 ± 1.46	2.67 ± 0.04	9.24 ± 0.12	0.940	FcµR-HVH5
HVH6	49.67 ± 1.33	2.82 ± 0.04	10.63 ± 0.12	0.944	FcµR-HVH6
HVH7	23.29 ± 0.36	4.97 ± 0.04	9.87 ± 0.10	0.942	FcµR-HVH7

Figure 2. BLI measurement of trastuzumab IgM variants (HVH1-7) interacting with FcµR bound to AHC biosensor. KD, k_a, k_d, R^2, and fitting curves are shown according to the 1:1 model. PR indicates poor responses where the measurements have a poor R^2 value are shown in red. The x-axis and y-axis of the graph represent time (s) and response (nM), respectively. All values are rounded off to 2 decimal places. Triplicate experiments were performed, and standard errors were reported

BIL measurements of pertuzumab and trastuzumab IgM variants to Her2

As a control for proper protein folding of IgM, two immobilisation methods: i) PpL binding to Vκ1 and ii) anti-IgM binding to the Fc region of IgM were used to evaluate the binding at the V-regions to the known antigen Her2 for KD measurement.

The measurements of the anti-IgM captured method (Figures 3 and 4) were more consistent than those of PpL-captured pertuzumab IgMs to Her2 (Figures 5 and 6), showing possible modulating effects from the PpL engagement.

Construct	KD (nM)	k_a (1/Ms) 10^4	k_d (1/s) 10^{-4}	R^2	
PVH1	PR	PR	PR	0.750	
PVH2	PR	PR	PR	0.603	
PVH3	4.61 ± 0.04	6.9 ± 0.03	3.18 ± 0.02	0.996	
PVH4	4.04 ± 0.21	4.49 ± 0.09	2.48 ± 0.06	0.953	
PVH5	32.57 ± 0.49	8.44 ± 0.12	27.45 ± 0.13	0.971	
PVH6	5.34 ± 0.25	4.87 ± 0.09	1.97 ± 0.06	0.970	
PVH7	10.17 ± 0.06	5.51 ± 0.02	5.59 ± 0.02	0.997	

Figure 3. BLI measurement of pertuzumab IgM variants (PVH1-7) interacting with Her2 using Anti-IgM bound on SA biosensor to capture the Fc region of IgM. KD, k_a, k_d, and R^2 and fitting curves are shown according to the 1:1 fitting model. The x-axis and y-axis of the graph represent the time (s) and response (nM), respectively. All values were rounded off to 2 decimal places. Triplicate experiments were performed, and standard errors are shown

Construct	KD (nM)	k_a (1/Ms) 10^4	k_d (1/s) 10^{-4}	R^2	
HVH1	PR	PR	PR	0.697	
HVH2	PR	PR	PR	0.811	
HVH3	4.97 ± 0.22	3.83 ± 0.05	1.36 ± 0.05	0.983	
HVH4	3.69 ± 0.11	4.08 ± 0.04	1.16 ± 0.04	0.992	
HVH5	6.37 ± 0.05	6.42 ± 0.03	3.86 ± 0.02	0.996	
HVH6	1.57 ± 0.05	6.54 ± 0.05	1.06 ± 0.03	0.992	
HVH7	5.06 ± 0.05	6.05 ± 0.03	3.00 ± 0.03	0.996	

Figure 4. BLI measurement of trastuzumab IgM variants (HVH1-7) interacting with Her2 using Anti-IgM bound on SA biosensor to capture the Fc region of IgM. KD, k_a, k_d, and R^2 and fitting curves are shown according to the 1:1 fitting model. The x-axis and y-axis of the graph represent the time (s) and response (nM), respectively. All values were rounded off to 2 decimal places. Triplicate experiments were performed, and standard errors are shown
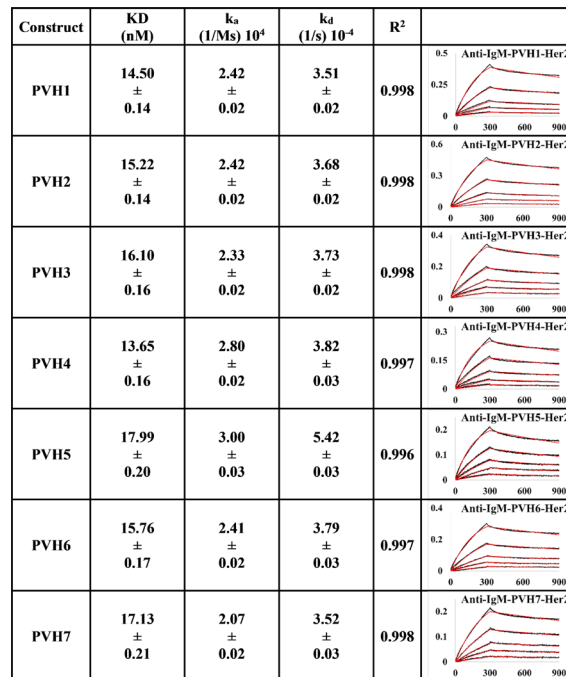
Construct	KD (nM)	k_a (1/Ms) 10^4	k_d (1/s) 10^{-4}	R^2	
PVH1	14.50 ± 0.14	2.42 ± 0.02	3.51 ± 0.02	0.998	Anti-IgM-PVH1-Her2
PVH2	15.22 ± 0.14	2.42 ± 0.02	3.68 ± 0.02	0.998	Anti-IgM-PVH2-Her2
PVH3	16.10 ± 0.16	2.33 ± 0.02	3.73 ± 0.02	0.998	Anti-IgM-PVH3-Her2
PVH4	13.65 ± 0.16	2.80 ± 0.02	3.82 ± 0.03	0.997	Anti-IgM-PVH4-Her2
PVH5	17.99 ± 0.20	3.00 ± 0.03	5.42 ± 0.03	0.996	Anti-IgM-PVH5-Her2
PVH6	15.76 ± 0.17	2.41 ± 0.02	3.79 ± 0.03	0.997	Anti-IgM-PVH6-Her2
PVH7	17.13 ± 0.21	2.07 ± 0.02	3.52 ± 0.03	0.998	Anti-IgM-PVH7-Her2

Figure 5. BLI measurement of pertuzumab IgM variants (PVH1-7) interacting with Her2 using PpL biosensor to capture the light chain of IgM. KD, k_a, k_d, and R^2 and fitting curves are shown according to the 1:1 fitting model. PR indicates poor responses where measurements with a poor R^2 value are shown in red. The x-axis and y-axis of the graph represent time (s) and response (nM), respectively. All values are rounded off to 2 decimal places. Triplicate experiments were performed, and standard errors were reported

Construct	KD (nM)	k_a (1/Ms) 10^4	k_d (1/s) 10^{-4}	R^2	
HVH1	17.08 ± 0.35	3.01 ± 0.05	4.77 ± 0.06	0.987	Anti-IgM-HVH1-Her2
HVH2	12.96 ± 0.21	3.12 ± 0.04	3.98 ± 0.04	0.993	Anti-IgM-HVH2-Her2
HVH3	1.16 ± 0.03	25.67 ± 0.25	2.54 ± 0.05	0.951	Anti-IgM-HVH3-Her2
HVH4	13.77 ± 0.15	2.45 ± 0.02	3.36 ± 0.03	0.998	Anti-IgM-HVH4-Her2
HVH5	13.68 ± 0.28	4.63 ± 0.07	5.63 ± 0.08	0.975	Anti-IgM-HVH5-Her2
HVH6	14.89 ± 0.15	2.28 ± 0.02	3.40 ± 0.02	0.998	Anti-IgM-HVH6-Her2
HVH7	5.90 ± 0.13	7.17 ± 0.10	4.23 ± 0.07	0.950	Anti-IgM-HVH7-Her2

Figure 6. BLI measurement of trastuzumab IgM variants (HVH1-7) interacting with Her2 using PpL biosensor to capture the light chain of IgM KD, k_a, k_d, and R^2, and fitting curves are shown according to the 1:1 model. PR indicates poor responses where measurements with a poor R^2 value are shown in red. The x-axis and y-axis of the graph represent time (s) and response (nM), respectively. All values are rounded off to 2 decimal places. Triplicate experiments were performed, and standard errors were reported
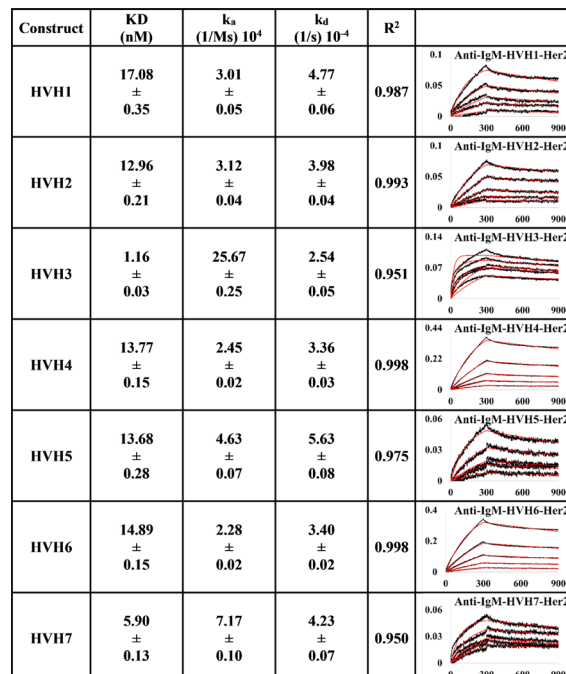
Anti-IgM immobilisation method showed that all pertuzumab (Figure 3) and trastuzumab (Figure 4) VH IgM variants bound to Her2. The pertuzumab variants showed a consistent KD value range between 13.65

nM and 17.99 nM, while the trastuzumab variants had KD values that ranged from 1.16 nM to 17.08 nM. While trastuzumab had better binders, both antibody models yielded a similar range of KDs. Ranking the best binders to the weaker ones, pertuzumab variants are in the order of PVH4, 1, 2, 6, 3, 7, and 5, while trastuzumab variants are ranked in the order of HVH3, 7, 2, 5, 4, 6, and 1. It is noteworthy that the specific VH families from pertuzumab or trastuzumab had similar KD values despite the different ranking order. Two notable exceptions are seen for VH families: VH3 and 7, where trastuzumab VH3 and 7 are ten- and three-folds better binders than pertuzumab VH3 and 7, respectively.

Using the PpL immobilisation method shown in Figures 5 and 6, VH1 and 2 FWRs, regardless of whether with pertuzumab or trastuzumab CDRs, failed to bind to Her2 antigen with R^2 values from 0.603 to 0.811. Generally, pertuzumab VH IgMs exhibited a more extensive range of KD values from 4.04 nM to 32.57 nM, compared to trastuzumab VH IgMs with KD values ranging from 1.57 nM to 6.37 nM. The best to the weakest binding IgMs for pertuzumab variants are in the order of VH4, 3, 6, 7, and 5, while for trastuzumab, the order is VH6, 4, 3, 7, and 5. Even though the interactions show that both pertuzumab and trastuzumab VH7 and 5 have the weakest interactions, the binding strengths of trastuzumab variants are still two to five-fold lower (better) than the pertuzumab variants.

Discussion

To investigate the effect of VH families on the FcµR engagement and that of antibody superantigen PpL in IgMs, 7 VH families were grafted to the CDRs of two well-studied cancer therapeutic antibodies, pertuzumab and trastuzumab. Previously, the VH FWRs were found to affect the CH-FcR interaction on other human antibody isotypes [14, 16, 17]. Here our panel of whole IgMs was made by recombinantly stitching the previous VH variants from the IgG1 pertuzumab and trastuzumab variants onto the human IgM CH [5] (Figure S1) that formed multimers consistent with other published work on IgM [3, 34, 35] and with our SEC analyses of selected samples (Figures S2 and S3) and preliminary EM-based characterization (Figure S4).

Since binding to the respective Ig FcRs determines the downstream immune cells' downstream activation, impaired receptor FcµR engagement by certain VH families, such as PVH2 and HVH1, can lead to lower efficacy in IgM therapeutics. Found on lymphocytes such as natural killer cells, B cells, and T cells [8–10], FcµR binds IgM at the CH [36]. In agreement with recent investigations that showed the V-regions (both VH and VL in combination) to influence FcR binding sites on the CH region for IgA [14, 15], IgE [16], IgG1 [17], similar effects were found here for IgM. From Figures 1 and 2, the best binders: PVH1 and HVH7 with 29.73 nM and 23.29 nM, respectively, had bindings to FcµR close to the reported literature of ∼10 nM [10, 37] affinity, albeit in a different system. Changing the VH families modulated the binding strength up to 9-folds.

Despite the lack of clear patterns for the effects of the VH-FWR families on FcµR-CH engagement on both pertuzumab and trastuzumab, combinatorial contributions from both CDRs and VH contributed to the effects of FcµR engagement since the pertuzumab CDR-grafted variants showed more pronounced effects than the trastuzumab CDR-grafted counterparts. Since the light chain within each antibody remained constant, it was assumed that they had minimum impact on the fluctuating KDs within pertuzumab when compared to trastuzumab IgM models.

While the measurements with Her2, FcµR, and PpL were part of our intended measurements in studying the effects of the VH families, the binding with these proteins also demonstrated that our IgMs were correctly folded at their respective binding regions to be recognized biophysically. In establishing possible avidity effects, both PpL (Vκ capture) and anti-IgM (IgM CH capture) immobilisation methods, where the successful loading of the IgMs by the two capture methods (Figure S5–S8) demonstrated correctly folding IgM binding sites that together with the SEC and preliminary EM results, gave us confidence that our IgMs were functional and folded correctly.

The two immobilisation capture methods also allowed investigations into the possible proximal modulation effect of superantigen PpL binding the Vκ FWRs on antigen engagement of Her2. Although trastuzumab and pertuzumab bind Her2 as their antigen, they had different epitopes that was previously shown to affect accessibility and cause steric clashes [6, 7] for IgM. It is thus reasonable to expect the binding

of superantigens [14, 38], particularly at the V-regions, to modulate antigen recognition due to the close packing of the V-regions for IgM to also result in steric clashes. It should be noted that the multimeric form of IgM locks the V-regions in spatial proximity, reducing the degrees of freedom of movement that would expectedly be further restricted by PpL binding.

Since antibody isotypes such as IgG1 were often immobilized at the Fc region using suitable capture proteins, e.g., Protein G in biophysical experiments to test the antigen binding affinity, we did not utilize natural antibody superantigens to capture the IgM Fc but used the two different capturing methods to measure the antigen binding affinity. From the PpL capture method (Figures 5 and 6), both pertuzumab and trastuzumab VH1 and VH2 gave poor responses to the Her2 antigen. Within the anti-IgM capture method (Figures 3 and 4), all the VH family variants bound to the Her2 antigen, including VH1 and 2. Such results showed that PpL binding to the VH1 and VH2 V-regions can abolish the binding to Her2. While this is due to the combinatorial effect of peculiar folding of specific VH-Vκ pairings, the findings provided an insight into the PpL immunomodulating the effects and the importance of the microbial superantigens from normal flora (discussed in [38] and [23]) which is expected to extend to other isotypes given the binding at the Vκ-FWR1 [21].

The log-fold difference between pertuzumab VH5 IgM and trastuzumab VH5 IgM within the PpL captured immobilisation results was in the same trend as the previously observed differences pertuzumab and trastuzumab IgG1s [4]. However, VH3 instead of VH5 IgM was seen with log-fold differences within the anti-IgM immobilisation results. Thus, holistically, PpL-captured IgM gave slightly better (lower) KD values than the anti-IgM capture method.

With the growing importance of IgM as a therapeutic antibody and its use in diagnostics (such as in haemagglutination kits), uncovering the mechanisms of these factors and how they can be mitigated by the presence of antibody superantigens and choice of FWR in CDR-grafting in humanisation [39] would be crucial for the efficacy of IgM for therapeutic and diagnostic uses.

Our panel showed the VH7 FWR to be a potential suitable FWR for CDR grafting for retaining binding strength for both the FcμR and antigen binding abilities. The amplification of the distal regional effects between the V- and C-regions due to the oligomerisation of IgM points to the need for future studies to investigate IgM candidates individually yet holistically to take into account the combinatorial factors involved. Such investigations would also need to include the effects of superantigens on antigen binding as found for IgEs and IgAs [5, 16]. Given that IgM is the primary response antibody, our findings here support the hypothesis that class-switching may be a mechanism for affinity maturation that ought to be considered during the humanisation step of antibody engineering [39].

In conclusion, we found exceptions within our recombinant IgMs that did not engage FcμR efficiently, likely caused by amplification of V-region distal effects on the C-region due to the oligomerisation. At the same time, the IgM CH was also found to influence antigen binding at the V-regions. With V-region superantigens such as PpL dampening antigen binding that the VH families could moderate, the interacting regions of the antibodies indeed demonstrate the complexity of IgM as an antibody format for future therapeutics showing the need for a personalised approach to antibody therapeutic development. In addition, our findings here support the use of CH engineering in antibody engineering, and that class switching may be a mechanism for affinity maturation in humans.

Abbreviations

BLI: bio-layer interferometry

Cat: Catalogue

CDRs: complementarity determining regions

CH: constant heavy

C-region: constant region

EM: electron microscopy

FcμR: Fc-mu receptor

FcR: Fc receptor

FWRs: framework regions

Her2: human epidermal growth factor receptor 2

Ig: immunoglobulin

J-chains: joining chains

k_a: association rate constant

KB: kinetic buffer

k_d: dissociation rate constant

KD: equilibrium dissociation constant

PpL: Protein L

SEC: size exclusion chromatography

VH: variable heavy

V-region: variable region

Vκ: variable region of the kappa light chain

Supplementary materials

The supplementary material for this article is available at: https://www.explorationpub.com/uploads/Article/file/100383_sup_1.pdf.

Declarations

Author contributions

WLL: Conceptualisation, Methodology, Investigation, Writing—Original Draft, Writing—Review & Editing. SKEG: Conceptualisation, Methodology, Investigation, Writing—Original Draft, Writing—Review & Editing, Funding Acquisition, Supervision. Both authors read and approved the submitted version.

Conflicts of interest

The authors declare that they have no conflicts of interest.

Ethical approval

Not applicable.

Consent to participate

Not applicable.

Consent to publication

Not applicable.

Availability of data and materials

The datasets GENERATED/ANALYZED for this study are available upon reasonable to the corresponding author (samgan@apdskeg.com).

References

1. Alberts B, Johnson A, Lewis J, Raff M, Roberts K, Walter P. Molecular biology of the cell. 4th ed. New York: Garland Science; 2002.

2. Cattaneo A, Neuberger MS. Polymeric immunoglobulin M is secreted by transfectants of non-lymphoid cells in the absence of immunoglobulin J chain. EMBO J. 1987;6:2753–8.

3. Fazel S, Wiersma EJ, Shulman MJ. Interplay of J chain and disulfide bonding in assembly of polymeric IgM. Int Immunol. 1997;9:1149–58.

4. Lua WH, Gan SKE, Lane DP, Verma CS. A search for synergy in the binding kinetics of trastuzumab and pertuzumab whole and F(ab) to Her2. NPJ Breast Cancer. 2015;1:15012.

5. Lua WH, Ling WL, Yeo JY, Poh JJ, Lane DP, Gan SKE. The effects of antibody engineering CH and CL in trastuzumab and pertuzumab recombinant models: impact on antibody production and antigen-binding. Sci Rep. 2018;8:718. Erratum in: Sci Rep. 2018;8:11110.

6. Samsudin F, Yeo JY, Gan SKE, Bond PJ. Not all therapeutic antibody isotypes are equal: the case of IgM *versus* IgG in pertuzumab and trastuzumab. Chem Sci. 2020;11:2843–54.

7. Gan SKE, Phua SX, Yeo JY. Sagacious epitope selection for vaccines, and both antibody-based therapeutics and diagnostics: tips from virology and oncology. Antib Ther. 2022;5:63–72.

8. Hancer VS, Diz-Kucukkaya R, Aktan M. Overexpression of Fc mu receptor (*FCMR, TOSO*) gene in chronic lymphocytic leukemia patients. Med Oncol. 2012;29:1068–72.

9. Honjo K, Kubagawa Y, Kubagawa H. Is Toso/IgM Fc receptor (FcμR) expressed by innate immune cells? Proc Natl Acad Sci U S A. 2013;110:E2540–1.

10. Kubagawa H, Oka S, Kubagawa Y, Torii I, Takayama E, Kang DW, et al. Identity of the elusive IgM Fc receptor (FcμR) in humans. J Exp Med. 2009;206:2779–93.

11. Honjo K, Kubagawa Y, Kearney JF, Kubagawa H. Unique ligand-binding property of the human IgM Fc receptor. J Immunol. 2015;194:1975–82.

12. Engels N, Wienands J. The signaling tool box for tyrosine-based costimulation of lymphocytes. Curr Opin Immunol. 2011;23:324–9.

13. Liu J, Wang Y, Xiong E, Hong R, Lu Q, Ohno H, et al. Role of the IgM Fc receptor in immunity and tolerance. Front Immunol. 2019;10:529.

14. Ling WL, Su CTT, Lua WH, Yeo JY, Poh JJ, Ng YL, et al. Variable-heavy (VH) families influencing IgA1&2 engagement to the antigen, FcαRI and superantigen proteins G, A, and L. Sci Rep. 2022;12:6510.

15. Su CTT, Lua WH, Ling WL, Gan SKE. Allosteric effects between the antibody constant and variable regions: a study of IgA Fc mutations on antigen binding. Antibodies (Basel). 2018;7:20.

16. Lua WH, Su CTT, Yeo JY, Poh JJ, Ling WL, Phua SX, et al. Role of the IgE variable heavy chain in FcεRIα and superantigen binding in allergy and immunotherapy. J Allergy Clin Immunol. 2019;144:514–23.E5.

17. Ling WL, Lua WH, Poh JJ, Yeo JY, Lane DP, Gan SKE. Effect of VH–VL families in pertuzumab and trastuzumab recombinant production, Her2 and FcγIIA binding. Front Immunol. 2018;9:469.

18. Phua SX, Chan KF, Su CTT, Poh JJ, Gan SKE. Perspective: the promises of a holistic view of proteins—impact on antibody engineering and drug discovery. Biosci Rep. 2019;39:BSR20181958.

19. Ling WL, Su CTT, Lua WH, Poh JJ, Ng YL, Wipat A, et al. Essentially leading antibody production: an investigation of amino acids, myeloma, and natural V-region signal peptides in producing pertuzumab and trastuzumab variants. Front Immunol. 2020;11:604318.

20. Heng ZSL, Yeo JY, Koh DWS, Gan SKE, Ling WL. Augmenting recombinant antibody production in HEK293E cells: optimizing transfection and culture parameters. Antib Ther. 2022;5:30–41.

21. Su CTT, Ling WL, Lua WH, Poh JJ, Gan SKE. The role of antibody Vκ framework 3 region towards antigen binding: effects on recombinant production and Protein L binding. Sci Rep. 2017;7:3766.

22. Su CTT, Lua WH, Poh JJ, Ling WL, Yeo JY, Gan SKE. Molecular insights of nickel binding to therapeutic antibodies as a possible new antibody superantigen. Front Immunol. 2021;12:676048.

23. Gan SKE, Derrick JP, Fraternali F. Editorial: understanding and engineering antibody-superantigen interactions. Front Immunol. 2022;13:857339.

24. Ling WL, Yeo JY, Ng YL, Wipat A, Gan SKE. More than meets the kappa for antibody superantigen Protein L (PpL). Antibodies (Basel). 2022;11:14.

25. Gasser R, Cloutier M, Prévost J, Fink C, Ducas É, Ding S, et al. Major role of IgM in the neutralizing activity of convalescent plasma against SARS-CoV-2. Cell Rep. 2021;34:108790.

26. Kober C, Manni S, Wolff S, Barnes T, Mukherjee S, Vogel T, et al. IgG3 and IgM identified as key to SARS-CoV-2 neutralization in convalescent plasma pools. PLoS One. 2022;17:e0262162.

27. Ku Z, Xie X, Hinton PR, Liu X, Ye X, Muruato AE, et al. Nasal delivery of an IgM offers broad protection from SARS-CoV-2 variants. Nature. 2021;595:718–23.

28. Shivarov V, Petrov PK, Pashov AD. Potential SARS-CoV-2 preimmune IgM epitopes. Front Immunol. 2020;11:932.

29. Lua WH, Ling WL, Su CTT, Yeo JY, Verma CS, Eisenhaber B, et al. Discovery of a novel splice variant of Fcar (CD89) unravels sequence segments necessary for efficient secretion: a story of bad signal peptides and good ones that nevertheless do not make it. Cell Cycle. 2017;16:457–67.

30. Phua SX, Lua WH, Gan SKE. Role of FcαR EC2 region in extracellular membrane localization. Cell Cycle. 2018;17:669–70.

31. Chan WT, Verma CS, Lane DP, Gan SKE. A comparison and optimization of methods and factors affecting the transformation of *Escherichia coli*. Biosci Rep. 2013;33:e00086.

32. Poh JJ, Gan SKE. The determination of factors involved in column-based nucleic acid extraction and purification. J Bioproces Biotechniq. 2014;4:157.

33. Hunt J, Harries HE, Gan SKE, Beavil AJ, Marsh PJ, inventors. The rapid expression of human immunoglobulins. Patent WO 2009/150426 A2. 2009 Dec 17.

34. Davis AC, Shulman MJ. IgM - molecular requirements for its assembly and function. Immunol Today. 1989;10:118–22, 27–8.

35. Wiersma EJ, Shulman MJ. Assembly of IgM. Role of disulfide bonding and noncovalent interactions. J Immunol. 1995;154:5265–72.

36. Skopnik CM, Al-Qaisi K, Calvert RA, Enghard P, Radbruch A, Sutton BJ, et al. Identification of amino acid residues in human IgM Fc receptor (FcμR) critical for IgM binding. Front Immunol. 2021;11:618327.

37. Kubagawa H, Honjo K, Ohkura N, Sakaguchi S, Radbruch A, Melchers F, et al. Functional roles of the IgM Fc receptor in the immune system. Front Immunol. 2019;10:945.

38. Deacy AM, Gan SKE, Derrick JP. Superantigen recognition and interactions: functions, mechanisms and applications. Front Immunol. 2021;12:731845.

39. Ling WL, Lua WH, Gan SKE. Sagacity in antibody humanization for therapeutics, diagnostics and research purposes: considerations of antibody elements and their roles. Antib Ther. 2020;3:71–9.